JOURNAL OF MODERN OPTICS, 2002, VOL. 49, NO. 3/4, 487–502

Electromagnetically induced opacity for photon pairs

K. J. RESCH, J. S. LUNDEEN and A. M. STEINBERG
Department of Physics, University of Toronto 60 St. George Street, Toronto, ON, M5S 1A7 Canada

(*Received 15 March 2001; revision received 17 May 2001*)

Abstract. It is shown that quantum interference with classical beams may be used to suppress or enhance the rate of spontaneous photon-pair production from a nonlinear crystal. Sum-frequency generation of the classical beams is simultaneously enhanced or suppressed via interference with a classical pump. In the extreme case, a crystal which is transparent to individual photons may block all photon pairs, converting them to 2ω. This constitutes a coherent nonlinear response at the single-photon level, enhanced by a factor of approximately 10^{10}. Experimental data and a theoretical description are presented, and an attempt is made to delineate the classical and quantum aspects of these effects.

1. Introduction

Many of the striking effects in atomic physics and quantum optics stem from atomic coherence and quantum interference. Electromagnetically induced transparency (EIT) [1] is an example of such an effect and has been the subject of numerous publications of late, as new related phenomena have been discovered. These new phenomena include slow light [2, 3] and 'stopped' light [4], as well as very large resonant nonlinear optical responses [3]. The schemes for producing these nonlinearities have not yet been extended to the single-photon level. One motivation for finding nonlinear responses for lower and lower light levels is the potential for applications to quantum information and computing. Performing quantum logic with propagating photons may have advantages over schemes relying on NMR [5], trapped ions [6], or high-Q optical cavities [7]. The major technical challenge is to make single photons, which generally interact very weakly, interact very strongly. One must use high intensity fields, on the order of $\mathrm{GW\,cm^{-2}}$, to produce reasonable nonlinear responses in conventional nonresonant nonlinear materials. This type of interaction is essentially negligible at the low intensities required for quantum computation. Recently, a single-photon nonlinearity has been reported [8] which is linked to the avalanche amplification stage in single-photon counting, and therefore cannot be considered a coherent nonlinearity. In this work, a coherent effective two-photon nonlinearity is described that may be useful for quantum information processing.

The scheme [9] relies on destructive interference between multiple Feynman paths that lead to the emission of a pair of photons. Multiphoton interference has been studied quite extensively in the past 15 years using sources of entangled photons (see, for example [10]), and more recently in systems with combinations of

Journal of Modern Optics ISSN 0950–0340 print/ISSN 1362–3044 online © 2002 Taylor & Francis Ltd
http://www.tandf.co.uk/journals
DOI: 10.1080/09500340110088623

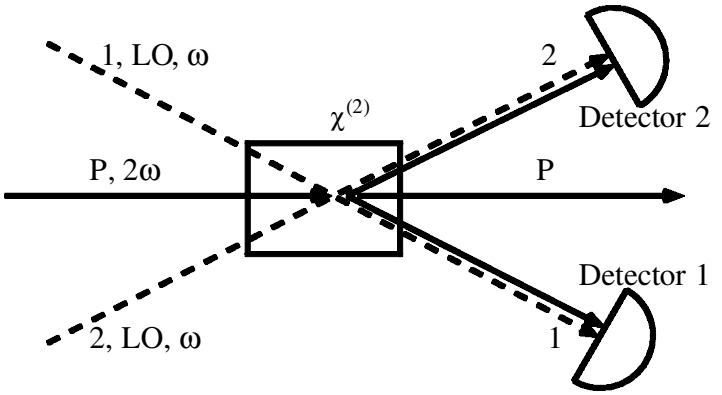

Figure 1. Simplified cartoon of the experiment. Pairs of weak coherent states in modes 1 and 2, at a frequency ω, are overlapped with the pairs of beams created via SPDC by the strong pump coherent state in mode p, at a frequency 2ω.

entangled sources and classical beams [11]. A greatly simplified schematic for our experiment is shown in figure 1. Mode 1 and mode 2 are initially populated by weak coherent states, and mode p contains a strong classical pump. The modes are chosen such that interaction with a nonlinear crystal with a nonzero $\chi^{(2)}$ allows spontaneous parametric down-conversion (SPDC) of the pump light into modes 1 and 2. To lowest order in the light intensity, there are two Feynman paths that can lead to a pair of photons in modes 1 and 2. Both coherent states can contribute a photon to make up a pair, or a pair can come from down-conversion. Experiment has shown that the phase information of the pump is not lost during down-conversion [12], and that even though the phase of one of the beams of down-converted light is random, it is strongly correlated to that of the other beam [13]. In effect, the phase of the pump laser is 'conserved' in the down-conversion process. It is this fact that allows a *pair* of laser beams to have a well-defined phase difference with the *pair* of down-converted beams. If the phase difference is chosen such that the two processes leading to the creation of a pair of photons after the nonlinear crystal interfere destructively, then photon pair production ceases. This effect is closely related to the 'railcross' experiment [14], in which suppression and enhancement of down-conversion was observed. In this work, independent beams are used instead of a closed interferometer, and it may be possible to use the parameters of those beams (i.e. polarization, intensity, frequency, phase) to observe new phenomena.

The only other proposals to observe nonlinear effects at the single-photon level for propagating beams are those involving photon-exchange interactions [15] and EIT [3]. The scheme presented in this work has some features in common with EIT-based systems and it is instructive to consider the relationship in some depth. Both systems rely on a strong coupling laser which is generally thought of as a spectator beam. The anomalous transmission in EIT, and two-photon 'absorption' in this scheme, are the results of interference between multiple pathways for processes involving the photons. In EIT, there are two ways that a photon can be absorbed to excite an atom. When the atoms are placed in the appropriate superposition of ground states, the two different absorption pathways that lead to an excited atom interfere destructively. Maintaining the proper phase relation-

ship between the two lasers is crucial for EIT. If the phase difference is abruptly changed, absorption will resume until the ground states evolve into a new coherent superposition with the right phase for transparency. In this scheme, as already stated, there are two ways for photon pairs to be emitted from the crystal which can be set to interfere destructively. As in EIT, the phase relationship between the pump laser and the pair of LOs is crucial to maintaining the destructive interference, or reduced two-photon emission becomes enhanced two-photon emission. In our case, the real transitions from EIT are replaced by virtual ones, and the susceptibility is modified by the pump, not by redistribution among real energy levels, but via nonresonant $\chi^{(2)}$ interactions.

2. Theory

A simple three-mode theory is included to describe the experimental schematic shown in figure 1. Weak coherent states begin in modes 1 and 2 with a frequency of ω. A strong pump coherent state at twice the frequency is in mode p. The pump laser can create pairs of photons in the nonlinear crystal through the process of SPDC, and those downconverted beams would be emitted into modes 1 and 2. The initial state of the system is a product of three different coherent states:

$$|\Psi(0)\rangle = |\alpha\rangle_1 \otimes |\beta\rangle_2 \otimes |\gamma\rangle_p, \tag{1}$$

where α, β, and γ are c-numbers labelling the coherent states in modes 1, 2, and p, respectively. In our experiment, α and β are much less than unity and describe the weak coherent states. γ, on the other hand, is much larger than unity and descibes the 'spectator' pump laser. If these fields are allowed to interact in a nonlinear crystal with a nonzero second-order susceptibility, $\chi^{(2)}$, then the state of the light will evolve by the interaction Hamiltonian

$$\mathcal{H}_{int} = g a_1^\dagger a_2^\dagger a_p + g^* a_1 a_2 a_p^\dagger, \tag{2}$$

which is comprised of field operators for the input modes, and the nonlinear coupling constant g which is proportional to the nonlinear susceptibility.

2.1. *Intensity of the light in modes p, 1 and 2*

First, we consider the rate of change in the intensities of the beams in modes p, 1 and 2. An expression for the time rate of change of the mean photon number in mode p can be calculated using the expression for the evolution of an expectation value:

$$\frac{\mathrm{d}}{\mathrm{d}t}\langle n_p\rangle = \frac{1}{\mathrm{i}\hbar}\langle [a_p^\dagger a_p, \mathcal{H}_{int}]\rangle \tag{3}$$

$$= \frac{1}{\mathrm{i}\hbar}\langle [a_p^\dagger a_p, g a_1^\dagger a_2^\dagger a_p + g^* a_1 a_2 a_p^\dagger]\rangle \tag{4}$$

$$= \frac{1}{\mathrm{i}\hbar}\langle g a_1^\dagger a_2^\dagger [a_p^\dagger a_p, a_p] + g^* a_1 a_2 [a_p^\dagger a_p, a_p^\dagger]\rangle \tag{5}$$

$$= \frac{1}{\mathrm{i}\hbar}\langle g a_1^\dagger a_2^\dagger (-a_p) + g^* a_1 a_2 a_p^\dagger\rangle \tag{6}$$

$$= -\frac{1}{\mathrm{i}\hbar}\langle g a_p a_1^\dagger a_2^\dagger - g^* a_1 a_2 a_p^\dagger\rangle. \tag{7}$$

The time rate of change of photon number in mode 1 can be calculated to be:

$$\frac{\mathrm{d}}{\mathrm{d}t}\langle n_1\rangle = \frac{1}{\mathrm{i}\hbar}\langle[a_1^\dagger a_1, \mathcal{H}_{int}]\rangle \tag{8}$$

$$= \frac{1}{\mathrm{i}\hbar}\langle[a_1^\dagger a_1, g a_1^\dagger a_2^\dagger a_p + g^* a_1 a_2 a_p^\dagger]\rangle \tag{9}$$

$$= \frac{1}{\mathrm{i}\hbar}\langle g a_2^\dagger a_p[a_1^\dagger a_1, a_1^\dagger] + g^* a_2 a_p^\dagger[a_1^\dagger a_1, a_1]\rangle \tag{10}$$

$$= \frac{1}{\mathrm{i}\hbar}\langle g a_1^\dagger a_2^\dagger a_p - g^* a_1 a_2 a_p^\dagger\rangle. \tag{11}$$

And similarly, the time rate of change of the photon number in mode 2 is,

$$\frac{\mathrm{d}}{\mathrm{d}t}\langle n_2\rangle = \frac{1}{\mathrm{i}\hbar}\langle g a_1^\dagger a_2^\dagger a_p - g^* a_1 a_2 a_p^\dagger\rangle. \tag{12}$$

Comparing these derivatives we see that:

$$\frac{\mathrm{d}}{\mathrm{d}t}\langle n_p\rangle = -\frac{\mathrm{d}}{\mathrm{d}t}\langle n_1\rangle = -\frac{\mathrm{d}}{\mathrm{d}t}\langle n_2\rangle. \tag{13}$$

As one would expect from energy conservation and the form of the interaction Hamiltonian, the rate of change in the photon number in mode p is equal in magnitude and opposite in sign to the rates of change of the photon numbers in modes 1 and 2. Since this is true to at all times, $\langle n_1 + n_p\rangle$ and $\langle n_2 + n_p\rangle$ are conserved to all orders. This is exactly the result we expect from second-harmonic generation, where two lower frequency photons, one from mode 1 and one from mode 2, are destroyed and a higher frequency photon is created in mode p.

We observe this effect by measuring the intensity of the beams in modes 1 and 2. If we time evolve our initial state, $|\Psi(0)\rangle$, under our interaction Hamiltonian, then to first-order, our state becomes:

$$|\Psi(\Delta t)\rangle = A\left[1 - \frac{\mathrm{i}\Delta t}{\hbar}(g a_1^\dagger a_2^\dagger a_p + g^* a_1 a_2 a_p^\dagger)\right]|\alpha\rangle_1 \otimes |\beta\rangle_2 \otimes |\gamma\rangle_p. \tag{14}$$

The normalization constant, A, is, in general, a complicated expression and since we will be concerned with ratios of terms, it is unnecessary to write out in full. However, in the relevant limits of weak coherent states in modes 1 and 2, and a strong coherent state in mode p, $A \approx 1/\sqrt{1 + (\Delta t/\hbar)^2|g|^2|\gamma|^2}$. Using the time evolved state, $|\Psi(\Delta t)\rangle$, we can calculate the mean photon number in mode 1, $\langle n_1\rangle$:

$$\langle n_1\rangle = \langle\Psi(\Delta t)|a_1^\dagger a_1|\Psi(\Delta t)\rangle \tag{15}$$

$$= |A|^2 \left\{ \begin{array}{c} \langle\alpha|_1 \otimes \langle\beta|_2 \otimes \langle\gamma|_p\left[1 + \frac{\mathrm{i}\Delta t}{\hbar}(g^* a_1 a_2 a_p^\dagger + g a_1^\dagger a_2^\dagger a_p)\right] \\ a_1^\dagger a_1\left[1 - \frac{\mathrm{i}\Delta t}{\hbar}(g a_1^\dagger a_2^\dagger a_p + g^* a_1 a_2 a_p^\dagger)\right]|\alpha\rangle_1 \otimes |\beta\rangle_2 \otimes |\gamma\rangle_p \end{array} \right\}. \tag{16}$$

After some algebra, we obtain the expression:

$$\langle n_1\rangle = |A|^2\left\{\begin{array}{l} |\alpha|^2 + \dfrac{\mathrm{i}\Delta t}{\hbar}\left[\begin{array}{l} g^*\alpha\beta\gamma^*(|\alpha|^2+1) + g\alpha^*\beta^*\gamma|\alpha|^2 \\ -g\alpha^*\beta^*\gamma(|\alpha|^2+1) - g^*\alpha\beta\gamma^*|\alpha|^2 \end{array}\right] \\ +\left(\dfrac{\Delta t}{\hbar}\right)^2\left\{\begin{array}{c} |g|^2|\gamma|^2(|\beta|^2+1)(|\alpha|^4+3|\alpha|^2+1) \\ +g^{*2}\gamma^{*2}\alpha^2\beta^2(|\alpha|^2+1) \\ +g^2\gamma^2\alpha^{*2}\beta^{*2}(|\alpha|^2+1) \\ +|g|^2(|\gamma|^2+1)|\beta|^2|\alpha|^4 \end{array}\right\} \end{array}\right\}. \tag{17}$$

We impose the usual approximation that g is a real coupling constant and impose the limits, $|\alpha| \ll 1$, $|\beta| \ll 1$, and $|\gamma| \gg 1$, on the coherent state labels. The expectation value can then be simplified to:

$$\langle n_1\rangle = |A|^2\left\{|\alpha|^2 + \frac{\mathrm{i}\Delta t}{\hbar}g(\alpha\beta\gamma^* - \alpha^*\beta^*\gamma) + \left(\frac{\Delta t g}{\hbar}\right)^2|\gamma|^2\right\}. \tag{18}$$

Since α, β, and γ are c-numbers, we can write them in terms of an amplitude and a phase, i.e. $\alpha = |\alpha|\exp(\mathrm{i}\varphi_\alpha)$, $\beta = |\beta|\exp(\mathrm{i}\varphi_\beta)$, and $\gamma = |\gamma|\exp(\mathrm{i}\varphi_\gamma)$. We make the definition $\Delta\varphi = \varphi_\alpha + \varphi_\beta - \varphi_\gamma$, then the expression for the expectation value can be written:

$$\langle n_1\rangle = |A|^2\left\{\left[|\alpha|^2 + \left(\frac{\Delta t g}{\hbar}\right)^2|\gamma|^2\right] + 2\frac{\Delta t}{\hbar}g|\alpha||\beta||\gamma|\sin(\Delta\varphi)\right\}. \tag{19}$$

The expectation value for the photon number in mode 2 can be calculated in a similar way as:

$$\langle n_2\rangle = |A|^2\left\{\left[|\beta|^2 + \left(\frac{\Delta t g}{\hbar}\right)^2|\gamma|^2\right] + 2\frac{\Delta t}{\hbar}g|\alpha||\beta||\gamma|\sin(\Delta\varphi)\right\}. \tag{20}$$

We can translate the expression for the expectation value of the singles rate in mode 1 into a visibility by taking the ratio of the oscillating term to the constant term in equation (19). This intensity visibility in mode 1, V_1, is given by:

$$V_1 = \frac{2\dfrac{\Delta t}{\hbar}g|\alpha|\,|\beta|\,|\gamma|}{|\alpha|^2 + \left(\dfrac{\Delta t}{\hbar}\right)^2|g|^2|\gamma|^2}. \tag{21}$$

Similarly, the visibility in the intensity at detector 2, V_2, is:

$$V_2 = \frac{2\dfrac{\Delta t}{\hbar}g|\alpha||\beta||\gamma|}{|\beta|^2 + \left(\dfrac{\Delta t}{\hbar}\right)^2|g|^2|\gamma|^2}. \tag{22}$$

In the experiment, we work in the limit where the probability of a photon from down-conversion is much less than the probability of a photon from a LO beam. In this limit, $|\alpha|^2 \gg (\Delta t/\hbar)^2|g|^2|\gamma|^2$, and the visibility is approximately:

$$V_1 \approx \frac{2\frac{\Delta t}{\hbar} g|\alpha||\beta||\gamma|}{|\alpha|^2} \tag{23}$$

$$= \frac{2\frac{\Delta t}{\hbar} g|\beta||\gamma|}{|\alpha|}. \tag{24}$$

If $|\alpha| \approx |\beta|$, the visibility is approximately the amplitude for down-conversion, which is much less than 1. However, if $|\beta|$ is much larger than $|\alpha|$, the visibility in the intensity of mode 1 becomes large. It is also apparent that both singles visibilities cannot be made arbitrarily large *at the same time*. Increasing the visibility at detector 1 will reduce the visibility at detector 2 in such a way that the product of their visibilities is roughly constant and much less than unity. In the first case studied in this experiment, the coherent states in modes 1 and 2 were approximately of equal intensity. In this regime, the singles visibility is expected to be very small as it is the ratio of the probability for down-conversion to unity. For a different set of parameters, the singles visibility was increased at one of the detectors by increasing the light intensity to the *other* detector.

This effect is exactly what one would expect classically. Light in modes 2 and p can, through difference frequency generation, create light into mode 1. The phase of this beam is the phase difference between the pump and the mode 2 beams, and therefore can interfere constructively or destructively with the LO passing through the crystal creating the intensity fringe pattern. Although the intensity of difference frequency generated is negligibly small, the amplitude modulations are enhanced through interference, in a manner analogous to homodyne detection. It is the interference between this very small amount of difference frequency and the weak LO beams that creates the measureable intensity modulations. The up-conversion efficiency is similarly enhanced as the immeasureably small amplitude of the up-converted light beats against the strong classical pump. This enhancement works out to be on the order of the number of photons per pump pulse. However, classical nonlinear optics cannot explain all of the effects observed in this experiment. In addition to monitoring the intensities in modes 1 and 2, we also monitor the coincidence rate between these two modes.

2.2. *Coincidence rate between modes 1 and 2*

We now consider the rate of coincidence detection, where photons are registered from the same laser pulse at the detectors in mode 1 and mode 2. The expectation value for the coincidence rate between modes 1 and 2 is given by:

$$\langle a_1^\dagger a_2^\dagger a_1 a_2 \rangle = \langle \Psi(\Delta t) | a_1^\dagger a_1 a_2^\dagger a_2 | \Psi(\Delta t) \rangle \tag{25}$$

$$= |A|^2 \left\{ \begin{array}{c} \langle \alpha |_1 \otimes \langle \beta |_2 \otimes \langle \gamma |_p \left[1 + \frac{\mathrm{i}\Delta t}{\hbar} (g^* a_1 a_2 a_p^\dagger + g a_1^\dagger a_2^\dagger a_p) \right] \\ \\ a_1^\dagger a_1 a_2^\dagger a_2 \left[1 - \frac{\mathrm{i}\Delta t}{\hbar} (g a_1^\dagger a_2^\dagger a_p + g^* a_1 a_2 a_p^\dagger) \right] |\alpha\rangle_1 \otimes |\beta\rangle_2 \otimes |\gamma\rangle_p \end{array} \right\}. \tag{26}$$

It can be shown that,

$$\langle a_1^\dagger a_2^\dagger a_1 a_2\rangle = |A|^2\left\{\begin{array}{c} |\alpha|^2|\beta|^2 \\ +\dfrac{\mathrm{i}\Delta t}{\hbar}\left\{\begin{array}{c} g^*\alpha\beta\gamma^*(|\alpha|^2+1)(|\beta|^2+1)+g\alpha^*\beta^*\gamma|\alpha|^2|\beta|^2 \\ -g\alpha^*\beta^*\gamma(|\alpha|^2+1)(|\beta|^2+1)-g^*\alpha\beta\gamma^*|\alpha|^2|\beta|^2 \end{array}\right\} \\ +\left(\dfrac{\Delta t}{\hbar}\right)^2\left\{\begin{array}{c} |g|^2|\gamma|^2(|\alpha|^4+3|\alpha|^2+1)(|\beta|^4+3|\beta|^2+1) \\ +g^{*2}\gamma^{*2}\alpha^2\beta^2(|\alpha|^2+1)(|\beta|^2+1) \\ +g^2\gamma^2\alpha^{*2}\beta^{*2}(|\alpha|^2+1)(|\beta|^2+1) \\ +|g|^2(|\gamma|^2+1)|\beta|^4|\alpha|^4 \end{array}\right\} \end{array}\right\}.$$

We invoke our assumption that g is real and impose the appropriate limits on the field labels:

$$\langle a_1^\dagger a_2^\dagger a_1 a_2\rangle = |A|^2\left\{\begin{array}{c} |\alpha|^2|\beta|^2 \\ +\dfrac{\mathrm{i}\Delta t}{\hbar}g[\alpha\beta\gamma^*(|\alpha|^2+|\beta|^2+1)-\alpha^*\beta^*\gamma(|\alpha|^2+|\beta|^2+1)] \\ +\left(\dfrac{\Delta t}{\hbar}\right)^2|g|^2|\gamma|^2 \end{array}\right\} \tag{27}$$

$$= |A|^2\left\{\begin{array}{c} \left[|\alpha|^2|\beta|^2+\left(\dfrac{\Delta t}{\hbar}\right)^2|g|^2|\gamma|^2\right] \\ +\dfrac{\mathrm{i}\Delta t}{\hbar}g(|\alpha|^2+|\beta|^2+1)|\alpha||\beta||\gamma|(\mathrm{e}^{-\mathrm{i}\Delta\varphi}-\mathrm{e}^{\mathrm{i}\Delta\varphi}) \end{array}\right\} \tag{28}$$

$$= |A|^2\left\{\begin{array}{c} \left[|\alpha|^2|\beta|^2+\left(\dfrac{\Delta t}{\hbar}\right)^2|g|^2|\gamma|^2\right] \\ +2\dfrac{\Delta t}{\hbar}g(|\alpha|^2+|\beta|^2+1)|\alpha||\beta||\gamma|\sin(\Delta\varphi) \end{array}\right\}. \tag{29}$$

In the low photon number limit, these oscillations have the same absolute size as the intensity oscillations; however, the constant term is reduced by a factor of $|\alpha|^2$ or $|\beta|^2$, both of which are much less than one in this limit. The visibility of such an effect can be expressed as a ratio of the oscillating term in equation (29) to the constant term. That visibility, V_c, is:

$$V_c \approx \frac{2\dfrac{\Delta t}{\hbar}g(|\alpha|^2+|\beta|^2+1)|\alpha||\beta||\gamma|}{|\alpha|^2|\beta|^2+\left(\dfrac{\Delta t}{\hbar}\right)^2|g|^2|\gamma|^2}. \tag{30}$$

In the limit for weak coherent states, this reduces to:

$$V_c \approx \frac{2\frac{\Delta t}{\hbar} g|\alpha||\beta||\gamma|}{|\alpha|^2|\beta|^2 + \left(\frac{\Delta t}{\hbar}\right)^2 |g|^2|\gamma|^2}. \tag{31}$$

The visibility of coincidence fringes is always larger than those in the intensity (equations (21) and (22)) in the appropriate limit of $|\beta| \ll 1$. The visibility in coincidence is 100% if $|\alpha|^2|\beta|^2 = (\Delta t/\hbar)|g|^2|\gamma|^2$, which is equivalent to setting the coincidence rate from downconversion equal to the coincidence rate from the LO beams. The depth of the modulations in the coincidence rate can be much larger than those in the singles and cannot be explained by classical nonlinear optics.

3. Experimental

To implement the scheme shown in figure 1 and discussed in the previous theory section, apparatus is set up as shown in figure 2. The light source is an ultrafast Ti:Sa laser operating with a centre frequency of 810 nm. A small amount of the light is removed from the laser at BS1 which will serve as the local oscillator (LO) beams, and the remainder of the light is frequency doubled in a β-barium borate (BBO) crystal to serve as the pump for down-conversion. The undoubled fundamental light is removed from the pump using coloured glass filters which allow only the second harmonic to pass. Two local oscillator beams are made by reducing the intensity of the light picked off from the laser and then rotating its polarization by 45°. The vertical polarization component of the resultant beam is one LO and the horizontal component is the other LO. These LO beams are then

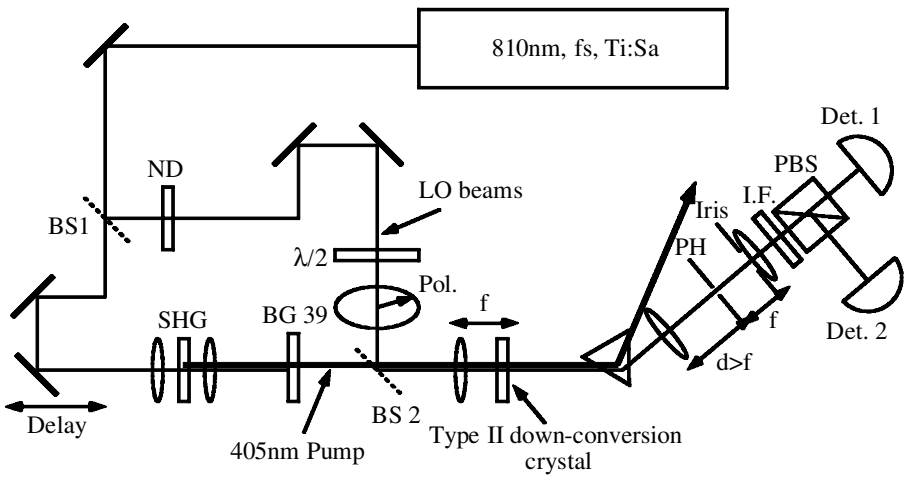

Figure 2. A schematic of the setup of the experiment. BS 1 and BS 2 are 90/10 (T/R) beamsplitters; SHG consists of two lenses and a BBO nonlinear crystal for type-I second harmonic generation; BG 39 is a coloured glass filter; ND is a set of neutral density filters; $\lambda/2$ is a zero-order half-wave plate; PH is a 25 µm diameter circular pinhole; I.F. is a 10 nm bandwidth interference filter, PBS is a polarizing beam splitter; and Det. A and Det. B are single-photon counting modules. The thinner solid line shows the beam path of the 810 nm light, and the heavier solid line shows the path of the 405 nm pump light.

recombined with the pump laser at BS2 and sent through the next nonlinear crystal. This second crystal is phase-matched for type-II collinear second harmonic generation (810 nm + 810 nm $\longrightarrow$ 405 nm), and hence is also phase-matched for the process of type-II collinear spontaneous parametric down-conversion (405 nm $\longrightarrow$ 810 nm + 810 nm). After the nonlinear crystal, a prism is used to separate the leftover pump light from the 810 nm beams (which now include the LO beams and the down-converted light). The 810 nm light is then passed through a spatial filter and an interference filter before getting split up by its polarization at the PBS and sent to two single-photon counting detectors (SPCMs).

In order for the laser and down-converted light to interfere, they must be made indistinguishable. Therefore they must have the same spatial modes, frequency bandwidth and time of arrival. The down-converted photons are inherently entangled in their spatial characteristics, frequency, and time of birth; these correlations must be removed, since they distinguish the down-converted pairs from the (unentangled) pairs from the laser beams. The arrival-time correlations are not an issue, as the pump and LO beams are all pulsed lasers. To ensure that the down-converted beams have the same spatial characteristics as the single spatial mode laser, all of the 810 nm light from the crystal passes through a simple spatial filter. The filter consists of a 25 μm diameter circular pinhole and a 2 mm iris approximately 5 cm downstream from the pinhole (figure 2). The light passing through the spatial filter is collimated by a 5 cm lens located directly after the iris. In order to achieve a high photon flux through this filter, the pump laser is focused onto the nonlinear crystal. This is related to a scheme designed to increase collection efficiency of photon pairs [16]. This created a smaller spatial source of down-conversion which could be imaged onto a much smaller spot at the pinhole. The pump focusing technique gives a factor of 30 higher coincidence rate than using a collimated pump laser. A 10 nm bandwidth interference filter with a peak transmission at 810 nm was included after the spatial filter for two reasons. The filter has a narrower bandwidth than the pump laser and therefore destroys any remaining frequency correlations between the pairs of down-converted beams, and also increases the overlap of the frequencies from the laser path and down-conversion path. The arrival time of the light pulses from the two different Feynman paths was controlled using a variable trombone delay in the pump path. Ensuring these three conditions merely makes the observation of interference a possibility. In order actually to observe interference fringes, the two Feyman paths must have a well-defined and controllable phase difference. The LO and pump beams are phase-locked by using the same laser source to produce them all. The phase difference is controlled using the optical delay in the pump path.

4. Results and Discussion

4.1. *Photon pair suppression and enhancement*

To look for the largest visibility effect in the coincidence rate between the SPCMs in modes 1 and 2, the coincidence rates from the LO beams alone were set to match the rates from the down-conversion path alone by using the appropriate number of ND filters in the LO arm. The coincidence counting rates were (3.3 ± 0.3) s^{-1} and (3.3 ± 0.3) s^{-1} from the LO Feynman path and the down-conversion paths alone. Owing to the uncorrelated photon numbers in the pair of LO beams, higher intensities are required to obtain the same coincidence rate as

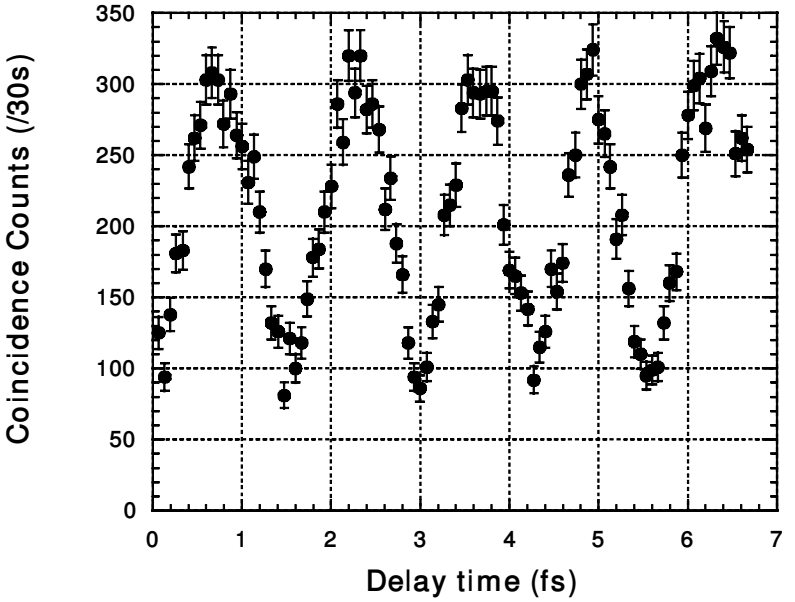

Figure 3. The coincidence rate as a function of the delay time. The interference is a phase-dependent enhancement or suppression of the photon pairs emitted from the crystal. The visibility of these fringes is $(47.4 \pm 0.9)\%$, and once corrected for background the visibility is 57%.

from down-conversion. For this reason, the singles rates from the LO beams are roughly 10 and 100 times higher than from the down-conversion for detectors 1 and 2, respectively. The optical delay was changed in the pump path, and the coincidence rate is shown as a function of that delay in figure 3. The visibility of the fringes in the coincidence rate is $(48 \pm 1)\%$, and if the background coincidence rate is subtracted that visibility is increased to 57%. The fringe period is about 1.3 fs/wavelength, which corresponds to a wavelength of approximately 405 nm. In equation (31), simple single-mode theory predicted that this visibility could be 100%. As with any interference pattern, the rate of events at the peak of a fringe is greater than the sum of the event rates from the two paths independently. This is an enhancement of the photon-pair production rate. A corresponding suppression of the photon-pair production occurs at the valley of a fringe. According to energy conservation, the reduction of the photon number in modes 1 and 2 at this point must be accompanied by an increase in the photon number in the pump mode, which occurs via enhanced sum-frequency generation.

4.2. *Phase dependent intensity modulation*

Theoretical treatment of this experiment showed that phase-dependent oscillations in the intensity should accompany the oscillations in the coincidence rates. It can also be seen, from these equations, that *both* LO beams are required in order to observe the modulations. If either α or β is zero, then the oscillating term vanishes. The laser light in the LO paths is polarized at 45° after the half-wave plate. Since the horizontal component of the polarization comprises the LO for detector 1 and the vertical component of the polarization comprises the LO for detector 2,

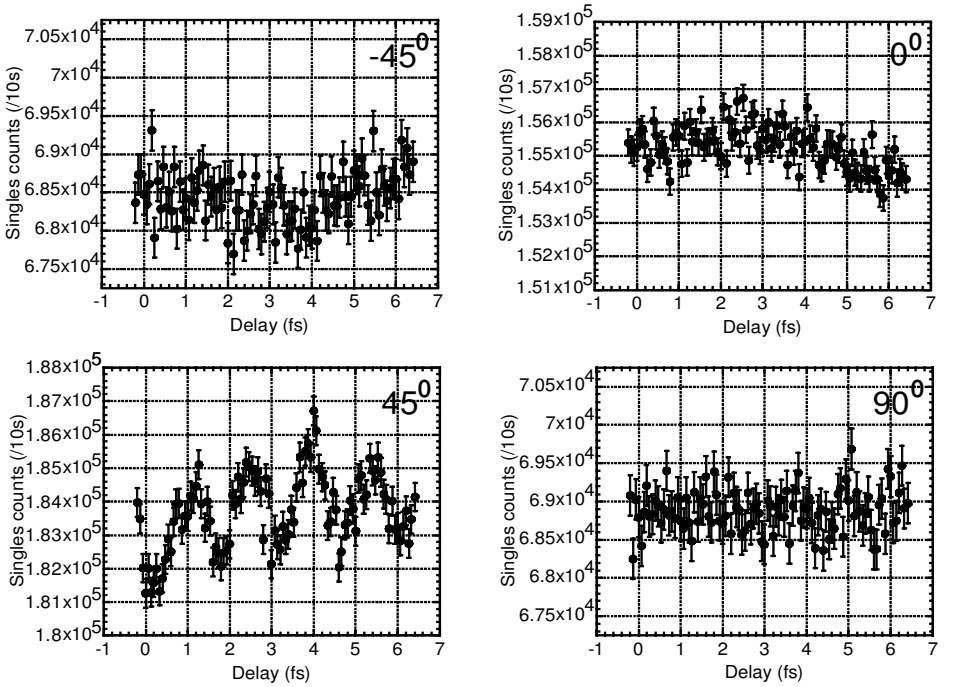

Figure 4. The singles rate at detector 1 versus the delay for four different polarizer angle settings. The left-hand data sets are for polarizer settings of ±45°. The right-hand column is for polarizer settings of 0° and 90°. The fringes are apparent only for the +45° polarizer setting, and have a visibility of 0.7% . These four data sets show that both horizontally and vertically-polarized photons must be present for the effect to occur.

blocking either or both of these polarization components should destroy the interference effect in the singles. It is obvious that blocking one of the LO beams should destroy the interference in the coincidence rate, as both LOs are required to obtain coincidence from the LO Feynman path. However, to show that blocking the LO beam that goes to detector 2 has an effect on the intensity of the LO for detector 1 is evidence for a nonlinear optical effect, and constitutes a coherent all-optical switch for single photons. Figure 4 shows the singles rate at detector 1 as a function of the delay time for four different polarizer settings. The left-hand column shows the diagonal basis settings where at -45° both LOs are blocked and at $+45^\circ$ both LOs may pass freely. Fringes at the 0.7% level are apparent in the singles rate only at 45° where both LOs could pass. The right-hand column of figure 4 shows the rectilinear polarization settings. Setting the polarizer at 0° or 90° only blocks a single LO beam, but this is sufficient to destroy the interference in the singles rate of detector A.

4.3. *Up-conversion of the local oscillator beams*

When destructive interference reduces the intensity of the beams reaching the detectors, energy conservation dictates that all incident laser photon pairs must be undergoing sum-frequency generation. Up-conversion is also predicted to occur by our single mode theory. At a fringe minimum in coincidences, we are also at a

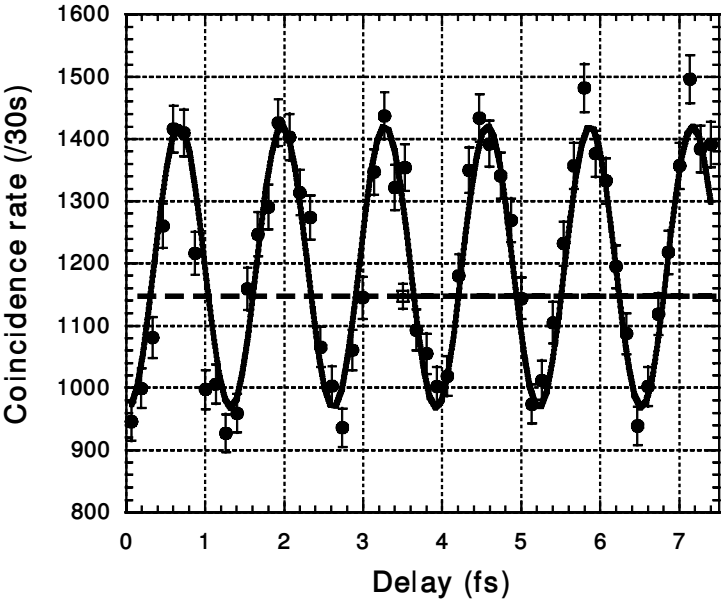

Figure 5. The coincidence rate versus the delay for a case where the rates from the different Feynman paths are severely imbalanced. This demonstrates that some photon pairs from the LO beams are being upconverted. The average value of the coincidence rate from the laser path alone is represented by a hollow square and the dashed horizontal line. The solid curve is a sinusoidal fit to the data. It is apparent for certain delay (phase) settings that the coincidence rate drops below the rate of coincidences from the LO paths alone. Based on the magnitude of this drop, it is concluded that at least $(15.7 \pm 1.7)\%$ of the photon pairs from the laser are upconverted.

minimum in singles and there is a predicted corresponding peak of equal absolute size in the pump photon number. Of course, this cannot be observed directly, given the background of approximately 10^{10} photons per pump pulse. To verify explicitly that photon pairs are actually removed from the LO beams, the reduction in the coincidence rate was measured relative to the coincidence rate from the LOs alone. In order to maximize the effect, the coincidence rates from the LO path and the down-conversion path were set to $(38.2 \pm 0.7)\ s^{-1}$ and $(1.2 \pm 0.2)\ s^{-1}$, respectively. The coincidence rate was again recorded as a function of the optical delay and is shown by the filled circles in figure 5. A sinusoidal fit to the data is shown as a heavy black line, and has a fringe visibility of $(19.0 \pm 0.5)\%$. The coincidence rate from the LO paths alone was measured before and after the experiment was performed and is shown as a horizontal dashed line, as well as an open square with error bars indicated. For delay positions where the solid black line drops below the dashed line, the photon pair detection rate drops below the value from the LO rate alone. This reduction in the pairs is due to photon pairs being removed from the LO beams undergoing sum-frequency generation. From the fringe visibility, we can infer that at least $(15.7 \pm 1.7)\%$ of the photon pairs from the local oscillator were converted into the second harmonic. This corresponds roughly to a few tenths of a per cent of the photons overall.

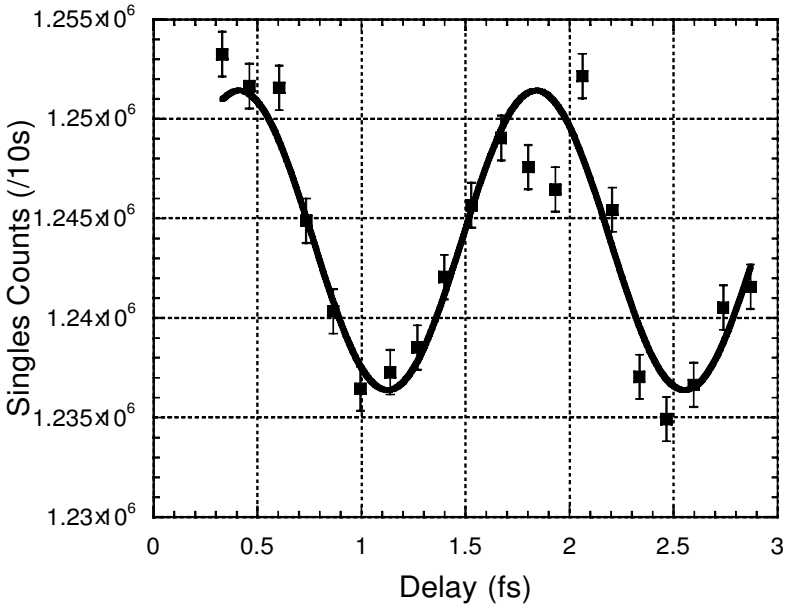

Figure 6. The singles rate at detector 2 versus the delay for a case where the coincidence rates from the two Feynman paths are severely imbalanced and the LO intensities are also imbalanced. At fringe minima, the intensity of the beam arriving at detector two is lower than one can account for by removing only down-converted photons.

In order to observe a similar effect in the intensity of light, the intensity of light in the LO beams was increased again. The coincidence rate was 2 s^{-1} from down-conversion and the singles rate at detector 2 was 371 ± 3 s^{-1} after background subtraction. The LO beam reaching detector 1 was too bright to measure directly; however, the counting rate could be inferred as approximately 8.3×10^5 s^{-1}. While this counting rate is comparatively large, it is still only 1 count per 100 pulses. The singles rate at detector 2 from the LO beam was 1.2×10^5 s^{-1}. The pump delay was changed to scan over a few fringes in the intensity at detector 2 and they are shown in figure 6. The fringe visibility was estimated from a fit of a subset of the data points to be $(0.61 \pm 0.06)\%$, which is a drop of (756 ± 74) s^{-1} below the average counting rate. This drop is too large to be from only the down-converted light by over 5σ, and therefore at least some of the photons from the laser must have been removed.

4.4. *Large-intensity oscillations*

Equation (22) describes the visibility in the intensity of mode 2 as a function of various experimental parameters. It can be seen that the visibility in the intensity of this mode can be increased by increasing the intensity of the light in the other mode. However, by comparing equation (22) for the intensity visibility, to equation (31), the visibility for coincidences, it is apparent that the singles visibility may approach the coincidence visibility as $|\alpha| \to 1$. To increase visibility in the singles rate of detector 2, the high intensity beam at detector 1 was used with approximately 8.3×10^5 s^{-1} and the maximum number of counts were extin-

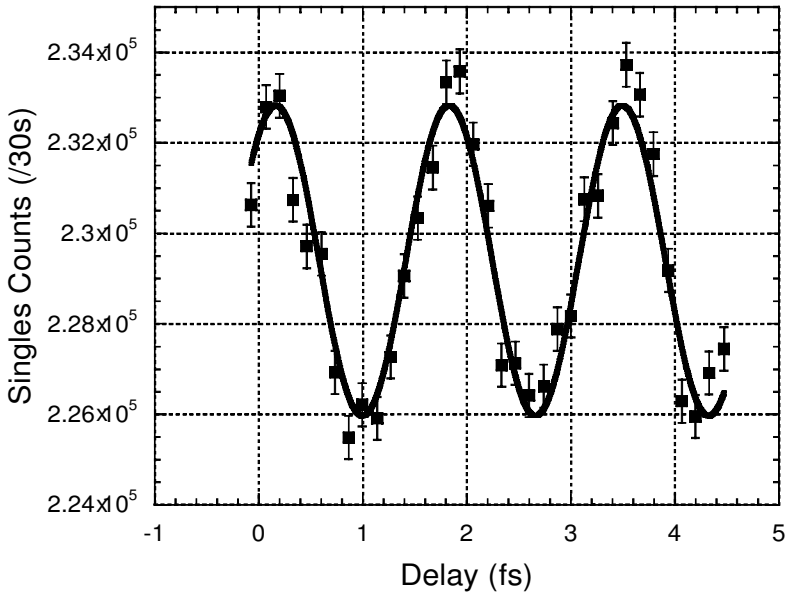

Figure 7. The maximum singles visibility—towards an optical switch for weak beams. The singles rate at detector 2 is shown as a function of delay. The visibility of the raw data is 1.5%, and is 2.6% once the background has been subtracted. The background-corrected visibility is 20% of the inferred coincidence visibility.

guished at Bob by use of the zero-order half-wave plate. This minimum rate was approximately 3500 s^{-1} once background had been subtracted, for an extinction of 1 part in 240. If we assume that the coincidence rate from the LOs is simply proportional to the product of the background free-counting rates at detectors 1 and 2, then the inferred coincidence rate was 37 s^{-1}. The coincidence rate from down-conversion was 2 s^{-1}. The maximum possible visibility in the coincidence rate is 44% based on the mismatch in the coincidence rates from the interfering paths. The coincidence visibility for this experiment was measured to be only (30 ± 4)% when the rates were balanced. Therefore, with the mismatched rates it can be inferred that the actual coincidence visibility would be roughly 44% of 30%, or 13.2%. The delay was scanned over fringes in the singles rate at detector 2 and are shown in figure 7. The raw visibility in this case is (1.50 ± 0.05)%, and after correcting for background the visibility is 2.6%. While this is not a very large visibility on its own, it is about 20% of the coincidence visibility which it cannot exceed. In the relevant limits, $V_c/V_2 \approx 1/|\alpha|^2$. Based on the singles rate at detector 1 one might infer $|\alpha| \approx 0.1$, which would give a ratio $V_c/V_2 \approx 100$ instead of the measured value of 5. This factor of 20 is attributed to a path efficiency of 5%. These results can be compared to those obtained for more balanced singles rates in the previous experimental sections. Under those experimental parameters, the singles visibility was approximately 0.7%, and the coincidence visibility was 57%. The singles visibility was only 1.2% of the coincidence visibility.

Detector (EG&G SPCM-AQ-131) breakdown impeded pushing this limit further. Achieving the high-visibility singles fringes necessary for optical switching of weak beams will be pursued in future work.

5. Conclusions

It has been shown, both theoretically and experimentally, that second harmonic generation can be greatly enhanced by the inclusion of a strong classical spectator field, due to interference. The enhancement is so large that the nonlinear crystal becomes effectively opaque to photon pairs in the low photon number limit. (This effect should not persist for higher mean photon numbers, as down-converted light is bunched relative to a coherent state.) The removal of photon pairs can also be seen as intensity modulations in those beams. The intensity modulations that were measured in the LO beams can be explained using classical nonlinear optics. Each of the weak LO beams can produce a small amplitude of difference-frequency light in the mode of the other LO. Through interference analogous to optical homodyning, that difference-frequency beam is greatly enhanced by beating against the LO beam, producing significant intensity modulations. Similarly, the immeasureably small sum-frequency amplitude generated by the pair of LO beams is enhanced by about 10^{10} by beating against the classical pump beam. Unfortunately, the presence of the strong pump makes it impossible to measure these oscillations directly. The modulations in the rate of coincidence detection cannot be explained in terms of classical nonlinear optics. The visibility in these oscillations was measured to be 57%, and in principle they can approach 100%. These can be understood as quantum interference between the two possible paths that lead to the detection of a pair of photons. Either both photons come from a down-conversion event, or one photon comes from each of the LO beams. Despite the uncertain phase of a *single* beam from SPDC, the phase of a down-converted photon *pair* of beams exhibits perfect quantum coherence with the pump. The interference between the amplitudes for these two processes gives rise to large coincidence modulations, even when the intensity modulations are quite low. It is this quantum interference that gives rise to the electromagnetically induced opacity. When the phase of the pump is chosen so that there is maximum destructive interference, the crystal becomes effectively opaque to photon pairs, and they are all upconverted into the pump laser beam.

Acknowledgments

We gratefully acknowledge funding from NSERC, CFI, Photonics Research Ontario, and the Walter C. Sumner Foundation.

References

[1] Harris, S. E., Field, J. E., and Imamoğlu, A., 1990, *Phys. Rev. Lett.*, **64,** 1107; Jain, M., Xia, H., Merriam, A. J., and Harris, S. E., 1996, *Phys. Rev. Lett.*, **77,** Lukin, M. D., Hemmer, P. R., Löffler, M., and Scully, M. O., 1998, *Phys. Rev. Lett.*, **81,** 2675; review in Harris, S. E., 1997, *Phys. Today*, **50,** no. 7, 36.

[2] Hau, L. V., Harris, S. E., Dutton, Z., and Behroozi, C. H., 1999, *Nature*, **397,** 594; Kash, M. M. *et al.*, 1999; *Phys. Rev. Lett.*, **82,** 5229; Kasapi, A., Maneesh, J., Yin, G. Y., and Harris, S. E., 1995, *Phys. Rev. Lett.*, **74,** 2447.

[3] Harris, S. E., and Hau, L. V., 1999, *Phys. Rev. Lett.*, **82,** 4611; Ham, B. S., and Hemmer, P. R., 2000, *Phys. Rev. Lett.*, **84,** 4080; Harris, S. E., 2000, *Phys. Rev. Lett.*, **85,** 4032; Lukin, M. D., and Imamoğlu, A., 2000, *Phys. Rev. Lett.*, **84,** 1419; Matsko, A. B. *et al.*, 2000, *Phys. Rev. Lett.*, **84,** 5752.

[4] Phillips, D. F., Fleischhauer, A., Mair, A., and Lukin, M. D., 2001, *Phys. Rev. Lett.*, **86,** 783.

[5] Gershenfeld, N. A., and Chaung, I. L., 1997, *Science*, **275,** 350; Jones, J. A., and Moscia, M., 1999, *Phys. Rev. Lett.*, **83,** 1050; Jones, J. A., Mosca, M., and Hansen, R. H., 1998, *Nature*, **393,** 344; Cory, D. G. *et al.*, 1998, *Phys Rev. Lett.*, **81,** 2152.
[6] Monroe, C. *et al.*, 1995, *Phys. Rev. Lett.*, **75,** 4714,
[7] Turchette, Q. A. *et al.*, 1995; *Phys. Rev. Lett.*, **75,** 4710; Nogues, G. *et al.*, 1999, *Nature*, **400,** 239.
[8] Resch, K. J., Lundeen, J. S., and Steinberg, A. M., 2001, *Phys. Rev. A*, **63,** 020102(R).
[9] Resch, K. J., Lundeen, J. S., and Steinberg, A. M., 2001, *Phys. Rev. Lett.*, **87,** 123603.
[10] Hong, C. K., Ou, Z. Y., and Mandel, L., 1987, *Phys. Rev. Lett.*, **59,** 2044; Ou, Z. Y., Wang, L. J., Zou, X. Y., Mandel, L., 1990, *Phys. Rev. A*, **41,** 566; Zou, X. Y., Wang, L. J., and Mandel, L., 1991, *Phys. Rev. Lett.*, **67,** 318; review in Mandel, L., 1999, *Rev. Mod. Phys.*, **71,** S264; Harihan, P., and Sanders, B. C., 1996, in *Progress in Optics*, vol. XXXVI, Emil Wolf, ed. (Amsteram: Elsevier), pp. 49–128.
[11] Rarity, J. G., Tapster, P. R., and Loudon, R., 1997, quant-ph/9702032.
[12] Koashi, K., Konon, K., Matsuoka, M., and Hirano, T., 1994, *Phys. Rev. A*, **50,** R3605.
[13] Kuzmich, A., Walmsley, I. A., and Mandel, L., 2000, *Phys. Rev. Lett.*, **85,** 1349.
[14] Herzog, T. J., Rarity, J. G., Weinfurter, H., and Zeilinger, A., 1994, *Phys. Rev. Lett.*, **72,** 629; Weinfurter, H., Terzog, T., Kwiat, P. G., Rarity, J. B., Zeilinger, A., and Zukowski, M., 1995, in Fundamental problems in quantum theory: a conference held in the honor of Professor John A. Wheeler, D. M. Greenberger and A. Zeilinger, eds (New York: The New York Academy of Sciences), pp. 61–72.
[15] Franson, J. D., and Pittman, T. B., 1999, *Phys. Rev. A*, **60,** 917.
[16] Monken, C. H., Souto Ribeiro, P. H., and Padua, S., 1998, *Phys. Rev. A*, **57,** R2267.